A Study of the Source Mechanism of the Alaska Earthquake and Tsunami of March 27, 1964

Part II. Analysis of Rayleigh Wave[1]

AUGUSTINE S. FURUMOTO

ABSTRACT: The source mechanism of the Alaska earthquake of March 27, 1964 has been investigated by analyzing the Rayleigh wave recorded on the strain seismograph at Kipapa Station, Hawaii. The parameters that give the best fit to the observed data are: rupture length of 800 km, rupture velocity of 3 km/sec, and direction of rupture line of S30°W. The results of this analysis compare favorably with field data of elevation changes, with distribution of epicenters of aftershocks, and with the area of generation of the tsunami as obtained from sea-wave refraction diagrams.

THE UNITED STATES–JAPAN Cooperative Field Survey of the Alaska Earthquake of March 27, 1964 (Berg et al., in preparation) resulted in an estimate of the length and size of the rupture zone of the earthquake. Corroboration for these results was sought from seismic data. Toksöz et al. (1965) have published a source mechanism analysis using surface wave data. Their results are as follows: rupture velocity, 3.0 km/sec; rupture length, 600 km; azimuth of rupture, S50°W from the epicenter. These results, however, are at variance with the field survey data.

Shortly after the field survey, an attempt at source mechanism analysis by surface wave methods was made by using the record of the strain seismograph at Kipapa Station, Hawaii. The results of this analysis are presented here because they are in somewhat better accord with field survey data.

This study was supported by funds from the National Science Foundation under Grants GP-2257 and GP-5111.

METHOD OF ANALYSIS

The analysis of source mechanism based on earthquake surface waves was developed by Ben-Menahem (1961). According to this method, if the Rayleigh wave is used the ratio of the amplitude spectrum of R_3 to the amplitude spectrum of R_2 can be related to directivity function D(f),

$$D(f) = \frac{\left|\left[\left(\frac{C}{V} + \cos\theta\right)\right] \sin\frac{\pi Bf}{C}\left(\frac{C}{V} - \cos\theta\right)\right]\right|}{\left|\left[\left(\frac{C}{V} - \cos\theta\right)\right] \sin\frac{\pi Bf}{C}\left(\frac{C}{V} + \cos\theta\right)\right]\right|} \qquad (1)$$

where C is the phase velocity of the curve at frequency f, V is the velocity of rupture propagation, B is the length of the rupture, and θ is the angle which the rupture line makes with the great circle path through the epicenter and observing station. A method using the Love wave has also been developed, but the present study utilizes the Rayleigh wave only.

Ben-Menahem and Toksöz have applied the method of surface wave analysis to the study of the source mechanism for the Mongolian earthquake of 1958 (Ben-Menahem and Toksöz, 1962), the Alaska earthquake of 1958 (Ben-Menahem and Toksöz, 1963*b*), and the Kamchatka earthquake of 1952 (Ben-Menahem and

[1] Hawaii Institute of Geophysics Contribution No. 185. Manuscript received June 22, 1966.

Toksöz, 1963*a*). Wada and Ono (1963) have applied the method for the Chile earthquake of 1960.

For the Alaska earthquake of 1964, copies of records from the strain seismograph at Kipapa Station, Hawaii, were used. This strain seismograph consists of a quartz rod 80 ft long. It was installed by the California Institute of Technology in the spring of 1963. Figure 1 shows the traces of R_2, R_3, and R_4.

RESULTS OF ANALYSIS

The Fourier spectra of R_2, R_3, and R_4 are given in Figure 2. To form the ratios of amplitudes R_3/R_2 and R_3/R_4, the decay of amplitudes with travel distance must be considered because the decay coefficient is frequency-dependent. The decay coefficient determined by Ben-Menahem and Toksöz (1963*a*) from empirical data was used for the corrections.

The amplitude ratios of R_3/R_2 and R_3/R_4 are given in Figure 3. There is coherence between the two ratio spectra at certain frequencies. Troughs of the spectra coincide at 0.0027 cps, 0.0056 cps, 0.0080 cps, and 0.0010 cps. Peaks agree at 0.0088 cps and 0.0111 cps. There is a peak at 0.0038 cps for R_3/R_4 and a peak

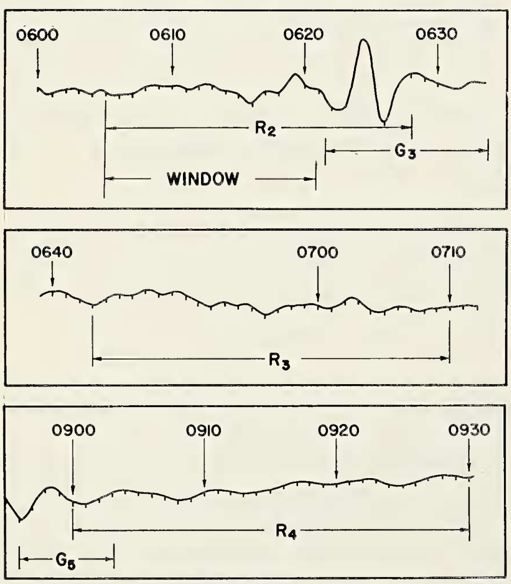

FIG. 1. *Upper*: Phases R_2 and G_3. Window indicates the section of R_2 that was used as data. *Middle*: Trace of R_3. *Lower*: Trace of R_4 and G_5.

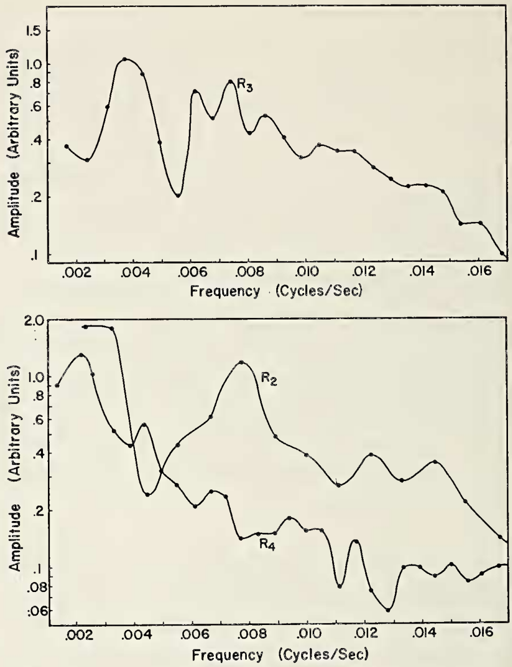

FIG. 2. *Upper*: Fourier spectrum of R_3. *Lower*: Fourier spectra of R_2 and R_4. The amplitude coordinate is in arbitrary units.

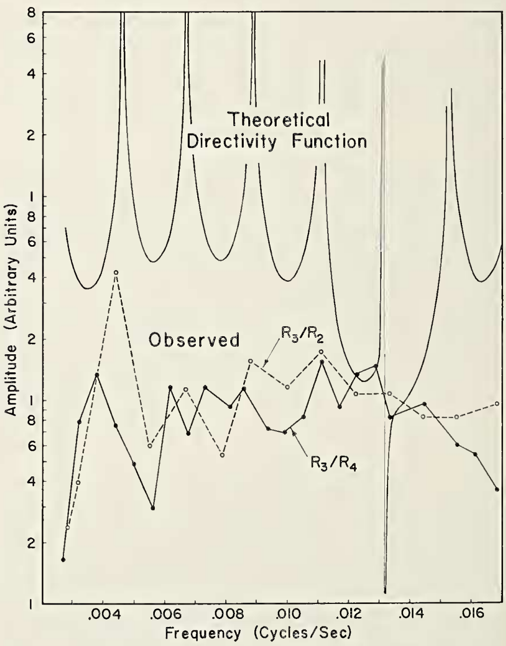

FIG. 3. Directivity function, theoretical and observed. The amplitude coordinate is in arbitrary units. For the theoretical curve, $V = 3$ km/sec, $\theta = 15°$, and $B = 800$ km.

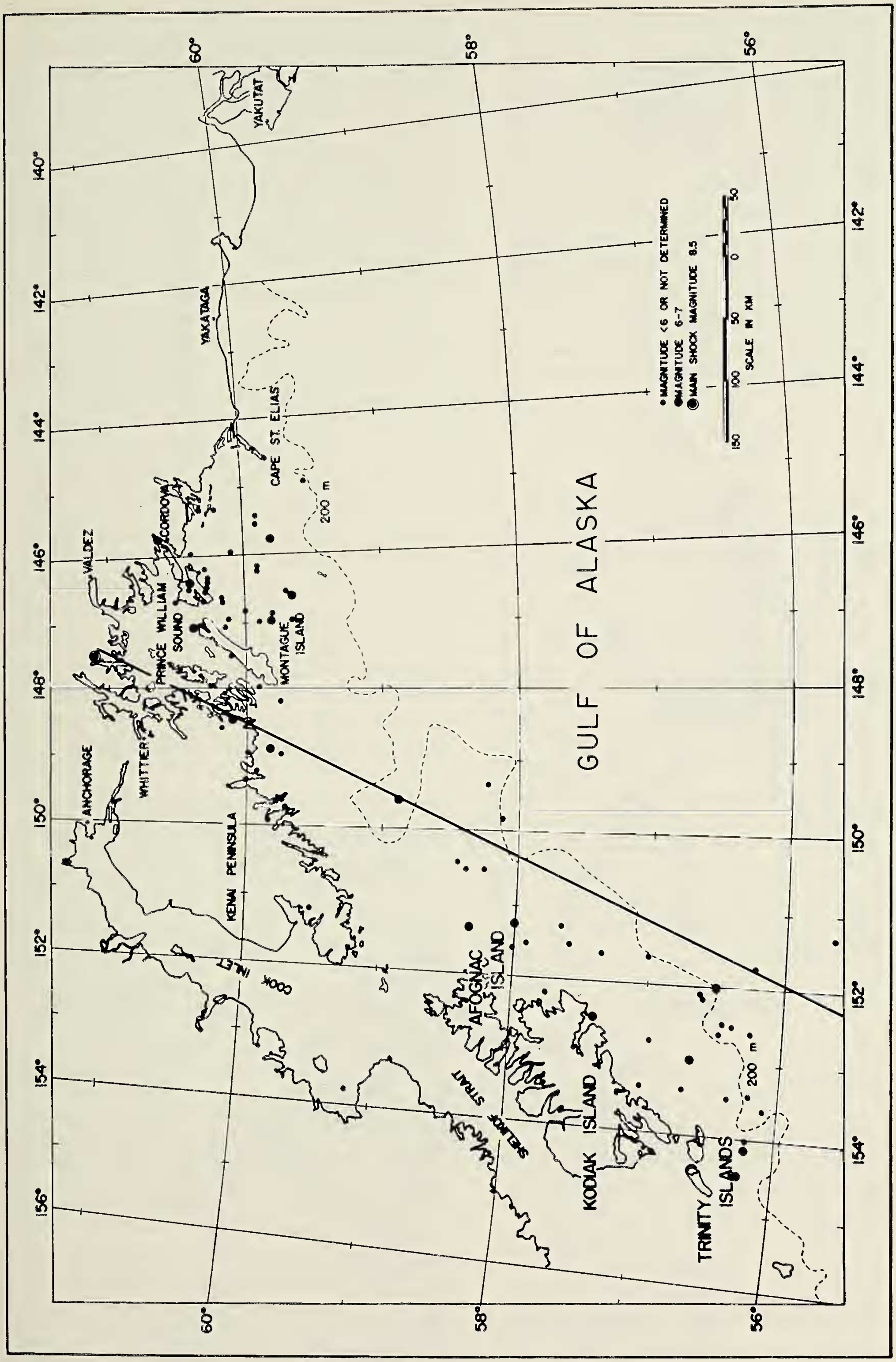

FIG. 4. The rupture line and distribution of epicenters of aftershocks.

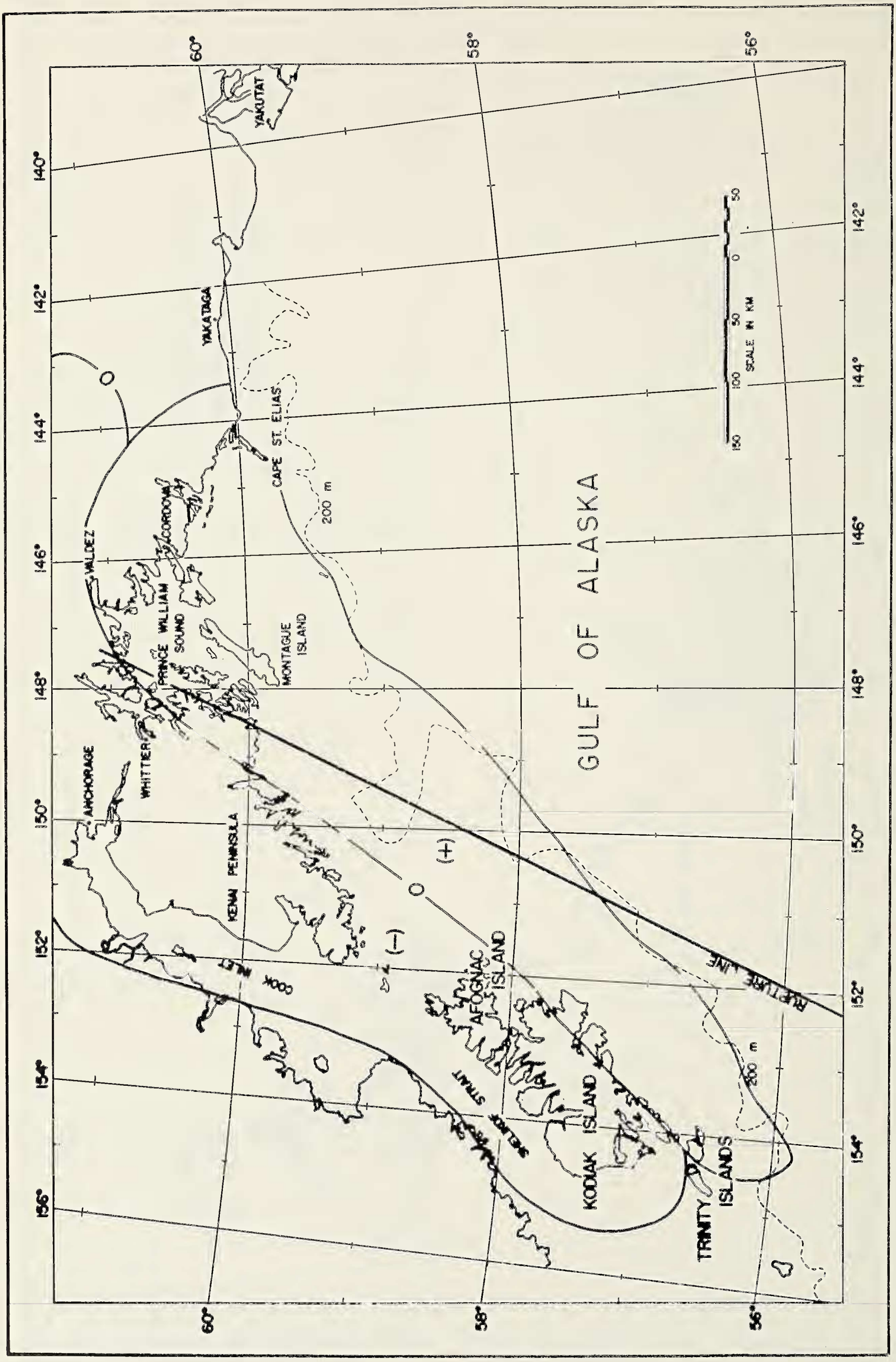

FIG. 5. The rupture line and elevation changes.

at 0.0044 cps for R_3/R_2. These two peaks probably coincide, and the apparent lag between the two is due to inadequate resolution of the Fourier analysis at these frequencies. There are opposing patterns at 0.0068 cps.

The best-fitting curve of the directivity function with the R_3/R_2 spectrum is plotted on the upper section of Figure 3. In this curve the parameters are: $B = 800$ km, $V = 3.0$ km/sec, and $\theta = 15°$. R_3/R_4 fits the curve also, except for the mismatch in the neighborhood of 0.0067 cps.

The epicenter determined by the U. S. Coast and Geodetic Survey (1964) was 61.05°N, 147.5°W. The coordinates of the Kipapa Station are 21°25′24″N and 158°00′54″W. The direction of the station from the epicenter is S15.3°W. This defines the direction of the rupture line from the epicenter as S30°W.

In Figure 4, the rupture line, as obtained from the present study, is superimposed on a map prepared by the U. S. Coast and Geodetic Survey (1964) which shows the epicenters of the main shock and the aftershocks of the Alaska earthquake. In general, the aftershock area defines the area of rupture. In the present case, the rupture line obtained from Rayleigh wave analysis extends 100 km beyond the aftershock area.

Surveys of elevation changes after the Alaska earthquake show positive changes in the Prince William Sound area, and negative changes in the Kodiak Island area. In Figure 5, the calculated line of rupture is superimposed on the map of elevation changes as prepared by Pararas-Carayannis (see his Fig. 1, on p. 302 of this issue). The rupture line runs diagonally across the section of positive changes. In this calculation the direction of the rupture line may vary about 5°. (This value is determined by the resolving power of the Fourier analysis.) If the direction of the rupture line is turned 5° clockwise, with the epicenter as the pivotal point, the rupture line will agree with the line of zero displacement from field observations.

An inspection of the directivity function D(f) in equation (1) shows that the periodicity in terms of frequency of the peaks and troughs of the function is controlled by the length B of the rupture line. The peaks and troughs of R_3/R_2 and R_3/R_4 in Figure 3 are such that a length of $B = 800$ km fits the data best. The superimposition of the rupture line on the elevation-change map shows that the rupture line extends to the south 100 km beyond the zone of elevation changes. On the other hand, if the total area of the observed elevation changes is considered, the zone has a length of 700–800 km (Plafker, 1965).

The present analysis shows a discrepancy between the direction of the calculated rupture line and the direction expected from field survey, but the discrepancy is within the limits of error of the calculation. The length of the calculated rupture line agrees with that from field data.

DISCUSSION

The results of the field survey by the United States–Japan Cooperative Team (Berg et al., in preparation) have heavily influenced the analysis presented here since the author was a member of the survey team. Perhaps because of this bias, the analysis should not be considered as an independent study but, rather, as additional evidence to strengthen the results proposed by the field survey. The rupture zone of the Alaska earthquake of 1964 has now been outlined consistently by four different methods: (a) field survey of elevation changes (Berg et al., in preparation; Plafker, 1965); (b) plot of epicenters of aftershock (U. S. Coast and Geodetic Survey, 1964); (c) tsunami refraction diagrams (Pararas-Carayannis, p. 301–310, in this issue); and (d) seismic surface wave method (this paper).

REFERENCES

BEN-MENAHEM, A. 1961. Radiation of seismic surface waves from finite moving sources. Bull. Seism. Soc. Am. 51:401–435.

——— and M. N. TOKSÖZ. 1962. Source mechanism from spectra of long period seismic surface waves, 1. The Mongolian earthquake of December 4, 1957. J. Geophys. Res. 67:1943–1955.

——— 1963*a*. Source mechanism from spectra of long period surface waves, 2. The Kamchatka earthquake of November 4, 1952. Ibid. 68:5207–5222.

——— 1963*b*. Source mechanism from spectra of long period seismic surface waves, 3. The Alaska earthquake of July 10, 1958. Bull. Seism. Soc. Am. 53:905–919.

BERG, E., D. C. COX, A. S. FURUMOTO, K. KAJIURA, H. KAWASUMI, and E. SHIMA. (In preparation.) Field Survey of the Tsunami of 28 March 1964 in Alaska. Hawaii Inst. Geophys., Rept. Series.

PLAFKER, G. 1965. Tectonic deformation associated with the 1964 Alaska earthquake. Science 148:1675–1687.

TOKSÖZ, M. N., A. BEN-MENAHEM, and D. HARKRIDER. 1965. Source mechanism of Alaska earthquake from long period seismic surface waves. (Abstr.) Trans. Am. Geophys. Union 46:154.

U. S. COAST AND GEODETIC SURVEY. 1964. Preliminary Report, Prince William Sound, Alaskan Earthquakes, March–April 1964. 83 pp.

WADA, T., and H. ONO. 1963. Source mechanism of the Chilean earthquake from spectra of long period surface waves. Zisin 16 (ser. II):181–187.